Title

Portable chemical detection platform for on-site monitoring of odorant levels in natural gas

Authors

Fung, Stephanie
Contreras, Raquel Pimentel
Fung, Alexander G
et al.

Publication Date

2023-08-01

DOI

10.1016/j.chroma.2023.464151

Peer reviewed

HHS Public Access

Author manuscript

J Chromatogr A. Author manuscript; available in PMC 2024 August 30.

Published in final edited form as:

J Chromatogr A. 2023 August 30; 1705: 464151. doi:10.1016/j.chroma.2023.464151.

Portable chemical detection platform for on-site monitoring of odorant levels in natural gas

Stephanie Fung[1,2], **Raquel Pimentel Contreras**[1], **Alexander G. Fung**[1,2,Ŧ], **Patrick Gibson**[1], **Michael K. LeVasseur**[1,2,¶], **Mitchell M. McCartney**[1,2,3], **Dylan T. Koch**[4,2], **Pranay Chrakraborty**[1,§], **Bradley S. Chew**[1,2], **Maneeshin Y. Rajapakse**[1,2], **Daniel A. Chevy**[4,2], **Tristan L. Hicks**[1], **Cristina E. Davis**[1,2,3,*]

[1]Department of Mechanical and Aerospace Engineering, University of California Davis, Davis, CA, USA

[2]UC Davis Lung Center, One Shields Avenue, Davis, CA 95616, USA.

[3]VA Northern California Health Care System, 10535 Hospital Way, Mather, CA 95655, USA

[4]Department of Electrical Engineering, University of California Davis, Davis, CA, USA.

Abstract

The adequate odorization of natural gas is critical to identify gas leaks and to reduce accidents. To ensure odorization, natural gas utility companies collect samples to be processed at core facilities or a trained human technician smells a diluted natural gas sample. In this work, we report a detection platform that addresses the lack of mobile solutions capable of providing quantitative analysis of mercaptans, a class of compounds used to odorize natural gas. Detailed description of the platform hardware and software components is provided. Designed to be portable, the platform hardware facilitates extraction of mercaptans from natural gas, separation of individual mercaptan species, and quantification of odorant concentration, with results reported at point-of-sampling. The software was developed to accommodate skilled users as well as minimally trained operators. Detection and quantification of six commonly used mercaptan compounds (ethyl mercaptan, dimethyl sulfide, *n*-propylmercaptan, isopropyl mercaptan, *tert*-butyl mercaptan, and tetrahydrothiophene) at typical odorizing concentrations of 0.1 – 5 ppm was performed using the device. We demonstrate the potential of this technology to ensure natural gas odorizing concentrations throughout distribution systems.

*Correspondence: cedavis@ucdavis.edu.
¶Presently at Photon, Inc.
Ŧ Presently at Profusa, Inc.
§Presently at Southern Arkansas University, Magnolia, AR 71753, USA

The authors declare the following competing financial interest(s): The authors declare that a patent application has been submitted on part of the work presented in this paper.

Keywords

Natural gas; odorants; mercaptans; gas chromatography; chemical sensors

1. Introduction

Natural gas is a major energy source in the U.S. making up 32% of the primary energy consumption [1]. Due to the potential dangers involved with natural gas leaks, there are federal regulations (49 CFR 192.625) in place that provision for the odorization of distribution-grade natural gas to a detectable concentration in air at one-fifth the lower explosive limit (LEL) such that humans would be able to detect a potential gas leak with a normal sense of smell [2]. Additionally, natural gas is largely comprised of CH_4, which has climate change impact potential that is 25 times greater than CO_2 [3]. The adequate odorization of natural gas is critical for the identification of gas leaks ensuring both the safe supply of this widely used energy source and prevention of greenhouse gas leakage. Sulfur containing odorant compounds [e.g., mercaptan compounds, tetrahydrothiophene (THT) and dimethyl sulfide (DMS)] are injected by pipeline operators and gas distribution companies to effectively odorize the gas [4].

It is critical to test distribution lines at varying points, as odorant concentrations can decrease due to oxidation of rusting pipes, adsorption onto pipes or appliances, and absorption into liquids [5]. Some gas distribution entities monitor the composition at waypoint stations that are midstream, but this does not guarantee the sufficient odorization of gas at points further downstream. Operators may opt to collect a sample of natural gas to test with standard analytical laboratory methods. These samples need to be analyzed within a certain time based on the sampling vessel used [6] and need to be sent to an outside lab if the gas distribution entity does not have in-house analytical capabilities. Additionally, standard analyses often only provide “total sulfur” readings. Such readings are inflated by the presence of sulfur compound impurities [7] found in natural gas lines, rather than providing individual concentrations of the added odorants.

Alternatively, pipeline operators may employ an ASTM standard (ASTM D6273 – 08) that outlines test methods for natural gas odor intensity. This method depends on the human sense of smell as the procedures call for a trained person to “sniff at the apparatus exhaust” to gauge odorization. However, odor thresholds vary from person to person [8], and this method is subject to biological factors such as odor fatigue or loss of smell. There are conditions that may result in olfactory impairment whether it is due to a condition or illness such as COVID-19 [9]. Overall, this industry sector needs capabilities for quantitative in-field monitoring of odorant compound levels throughout all points of distribution.

Previous work by our team showed promising results for a modular open-source platform taking commercially available parts and integrating them into a modular and reconfigurable system to measure volatile organic compounds (VOCs) [10,11]. Building upon the previous work, a new platform is presented with hardware and software specifically designed and tailored to target natural gas odorant detection. The resulting device is the first of its kind, providing sample-to-analysis odorant concentration monitoring suitable for mobile

deployment. The main objectives of this work are to (1) develop a natural gas odorant monitoring platform suited for mobile deployment, and to (2) demonstrate speciation of the odorant compounds as a proof of concept.

2. Materials and Methods

2.1. Platform Software and Hardware

The detection platform is an integration of custom software and a hardware system as depicted (Figure 1). The custom software (2.1.1) is comprised of embedded microcontroller code and a Python-based graphical user interface (GUI) program. The hardware system (2.1.2) facilitates the extraction of mercaptans from natural gas, the separation of individual mercaptan species, and detection/quantification of odorant compounds in a single device.

2.1.1. Custom Software—There are two principal components that make up the platform software: the embedded microcontroller code and the GUI. The embedded microcontroller code runs on an Arduino based development board (Teensy 3.6). The embedded code facilitates all the hardware functions of the flow system. Digitized readings from the sensors and the detector are saved as an interaction between the embedded code and the GUI. Tables summarizing the microcontroller communication protocols are provided as supplemental material (S1).

The GUI is a Python-based program that provides the operator with capabilities to control the hardware and to perform analysis on natural gas samples. The method is set through the GUI and is transmitted to the microcontroller, executing the sequence of events automatically. Subsequently, detector data is streamed to the GUI and from this data, an odorant concentration estimation is produced based on the data analysis method described. Each of the tabs of the GUI are shown in supplemental material (S2).

2.1.2. Hardware System—The device has been arranged into three layers as depicted in the exploded 3D model (Figure 2). The system hardware is largely comprised of commercial off the shelf components which are detailed in supplemental material (S3). The frame for the system is constructed from laser cut acrylic panels and standard fasteners. The custom electronics are implemented with printed circuit boards (PCB) that were designed in KiCad and the circuit schematics are available as supplemental material (S4). The device dimensions are 300 × 290 × 290 mm and 6 kg. In the following sub-sections, key hardware components are described in detail organized by layer.

2.1.2.1. Layer I: Flow Control: The components responsible for sampling and control of the desorption and supplemental nitrogen flow are positioned on **Layer I** of the device. The system manages the distribution of the sample through the analysis components and the control of the supplemental carrier gas throughout the device. The sample can be drawn directly from a natural gas line regulated down to less than 1 psi or from a sample vessel (e.g., Tedlar bag or inert canister). The sample pump (KNF, NPM015) (Figure 2, 11) is connected to either the sample inlet or atmosphere through a 3-way valve (Clippard, NR1-3M-12) (Figure 2, 9). The sample flow rate is manually controlled downstream through a needle valve (Swagelock, SS-SS2) (Figure 2, 7) and is measured by a natural

gas flow sensor (OMRON, D6F-01N2-000) (Figure 2, 6). The supply of ultra-high purity (UHP) nitrogen gas (AirGas, UHP300) (Figure 2, 18) is introduced through a pressure regulator (McMaster, 6763K81) (Figure 2, 17). The regulator protects the downstream components that have specified pressure limits. Moreover, the UHP nitrogen goes through an additional filter (Valco, ZUFR2) (Figure 2, 16) to prevent particles larger than 2 mm from reaching sensitive components. The overall system flow rate of nitrogen is controlled by a proportional valve (Norgren, D170.0004) (Figure 2, 14). A flow sensor (Honeywell, HAFBLF0750C4AX5) (Figure 2, 13) provides feedback for overall flow control. At the proportional valve (Norgren, D170.0004) (Figure 2, 12), the system flow splits into two branches: the desorption flow and the make-up flow. The desorption flow carries the sample through the analysis components. The make-up flow supplements the desorption flow into the detector. This supplemental flow is modulated by another needle valve (Figure 2, 15), enabling the proportional valve control of desorption flow to operate within a specified range.

2.1.2.2. Layer II: Analysis: Layer II contains the elements of the system related to heating and sample analysis. The sorbent-packed trap (Figure 2, 3) between the 3-way valves (Clippard, NR1-3M-12) (Figure 2, 4 & 21) is used to extract the odorant compounds from natural gas samples allowing for larger sampling volumes while retaining odorant compounds on the silica gel sorbent. For the work herein, a trap packed with silica gel sorbent was used. The sorbent traps are constructed with a stainless-steel tube that has been treated with Sulfinert® (SilcoTek, Bellefonte, PA) which passivates the tubing surface with a layer of amorphous silicon to prevent degradation of sulfur compounds with the trap housing during heating. The construction for the trap component is a modified version of the heated line devices as described in supplementary material (S6). Before the fittings are placed, silica gel sorbent is packed into the device and held in place by steel mesh frits.

Gas chromatography (GC) is used to separate the individual odorant compounds. The transit of the sample and the resultant retention peaks strongly depend on the temperature profile from sampling to detection. Due to this, the entire analysis flow path is typically housed in a high-power GC oven. This presents a challenge for mobilizing GC capabilities in a portable device.

This challenged is addressed by utilizing controlled directed heating to the critical flow paths. For the GC column, a “low thermal mass” (LTM) GC column, type DB-624, 30 m × 0.32 mm × 1.80 μm (Agilent, 123-1334LTM) (Figure 2, 5) is employed. These commercially available GC modules provide “ultrafast temperature programming with an unprecedented cool down time and low power consumption” [12] that is characteristic of Low Thermal Mass Gas Chromatography (LTMGC). For the sample flow paths entering and exiting the GC column, heated line devices were constructed in-house to directly heat the critical flows. There are a total of three heated line devices that are set to hold at a constant temperature of 100 °C. The construction method for the heated line devices is included as supplemental material (S6). The first connects the sorbent trap to the GC, heating the GC inlet flow. The remaining two heated line devices are assembled on a make-up adapter (Valco, MUA) where one heats the nitrogen at the supplemental make-up flow inlet and the other heats the body of the make-up adapter that connects the outlet of the GC column to the inlet of the detector

(Figure 2, 20). Additionally, the detector is also heated to a constant temperature with a heater constructed of resistive wire embedded into silicone.

The differential mobility spectrometry detector (Figure 2, 20) is a custom in-house device that measures mercaptans through a physical interaction of the chemical compound and the detector electrodes. It operates off the principal of ion mobility, whereby mercaptan ions are manipulated in a drift tube with oscillating, asymmetric energy fields, then interacting with the detector pad to generate the chemical signal [13,14]. The detector runs off a single 12 V supply allowing for it to be operated as a standalone device or as in this work, a platform integrated detection module. Separation waveforms are generated by the Boost Converter and RF Amplifier controlled in tandem by several digital potentiometers. The circuit schematics and explanation of the electronics are detailed in supplemental material (S7).

The detection electronics and the sensor chip are an adaptation of the work previously described fully in [15]. The main physical modification is the location of the ultra-violet (UV) ionization source which was relocated to bottom of the fixture. This required an opening to be drilled in the bottom glass plate of the detector flow path to allow UV light to pass through for ionization. The drawing included in supplementary materials (S 7-5) illustrates the modifications for the sensor chip in this work compared to the chip in [15].

2.1.2.3. Layer III: Power: The power distribution architecture was designed to enable mobile deployment of the platform. A compact computer power supply (EVGA SuperNOVA 450 GM) serves as the main power supply and is integrated into the chassis. This supply provides a robust source for commonly required voltage levels for the system while allowing the device to be powered by a single standard AC power cord. A PCB facilitates power distribution to the various platform modules, and the circuit schematic is available as supplementary material (S 4-1). Powering the UV bulb ionization source posed a unique challenge as high voltage levels (>1 kV) are required to ignite the bulb. The High Voltage Power Supply (HVPS) module was designed to address those requirements. The HVPS is an isolated module that powers the bulb safely while mitigating potential electromagnetic interference (EMI). In addition to a manual switch, the HVPS can be controlled digitally so that the main controller electronics can power the ionization source on and off removing the need for physical contact with the high voltage electronics. The circuit schematic for the HVPS is provided as supplemental information (S 4-2).

2.1.3. System Operation—The device is adapted to handle a variety of potential applications, as natural gas can be sampled either directly from a regulated source or a containment vessel. Once attached to the device inlet, the sample pump pulls the sample concentrating the odorant onto the sorbent trap. The needle valve downstream of the trap augments the flow rate of sampling collection. The sampling time is set through the platform GUI software providing a tunable device sensitivity parameter.

After the sampling phase is completed, the system goes into the analysis phase during which a pressurized nitrogen gas cylinder drives the system flow. The phase begins with the trap heated to the desorption temperature whereby the nitrogen flow carries the released sulfur

compounds to the GC column. The desorption flow is increased initially as the trap is heated to desorb the pre-concentrated sample from the trap. Then the desorption flow is held at a lower flow rate for the rest of the analysis period. Following the GC column, a fused silica make-up adapter (VICI, Houston, TX) connects the column to the detector module. The adapter facilitates the introduction of a nitrogen auxiliary flow for the compounds as they elute from the GC column and into the detector module. The rates of the GC flow and make-up flow are set by a combination of two proportional valves and a manual needle valve. The two proportional valves are electronically controlled allowing for a control scheme to be implemented in the embedded software. After the analysis phase is complete, the raw data is processed by the GUI, which provides the quantitative concentration values for individual mercaptan species.

2.2. Analytical method

Distribution lines are odorized with approximately 1 ppm concentration mercaptans [16], which was used as the target concentration for optimization. Prior to development of this custom mercaptan sensor, certain analytical parameters occurred on a commercial platform to achieve target mercaptan sensitivities with minimal sampling times. Select optimization parameters are included as supplemental material (S5). The following method was used on the mercaptan sensor.

At initiation of sample collection (t=0 s), the silica gel trap was held at 35 °C, sampling for 60 s at a rate of 60 mL/min. The trap was then flushed with ambient air for 5 s to purge residual natural gas from the trap. Desorption occurred at t=67 s after sample collection was initiated and was achieved by heating the trap to 180 °C for 170 s (until t=237 s). A 5 mL/min flow of ultra-high purity nitrogen carried desorbed mercaptans from the trap and through the GC column, which was maintained at 40 °C throughout desorption. At t=127 s, the flow through the GC column was reduced to 1 mL/min. At t=1045 s, the GC column was then heated to 160 °C at a rate of 25 °C/min, holding until 1650 s.

The GC column eluent was mixed with a 600 mL/min auxiliary flow of nitrogen into the ionization and detector module. The detector fixture was set to 35 °C and scanned from −2 to 2 compensation voltage (CV) with the separation voltage (SV) set to 0 V to maximize sensitivity.

2.2.1. Standards and Sample Preparation—Odorant samples were prepared by diluting pure mercaptan standards in 10 L Tedlar bags with nitrogen balance at precise concentrations. Commercial standards of ethyl mercaptan (ETM), dimethyl sulfide (DMS), *n*-propylmercaptan (NPM), isopropyl mercaptan (IPM), *tert*-butyl mercaptan (TBM), and tetrahydrothiophene (THT) were purchased from Sigma-Aldrich (Burlington, MA). Ultra-high purity nitrogen gas was obtained from AirGas (Radnor Township, PA). Tedlar bags were from Restek Corporation (Bellefonte, PA).

The ideal gas law was used to calculate the required liquid volume from the original vials for preparation of the stock mixture concentration of 1000 ppm v/v in nitrogen balance. Serial dilutions were made using additional Tedlar bags to achieve target concentrations.

2.2.2. Sensor calibration and data analytics—Data generated by the detector is three dimensional, with the x-axis representing compensation voltage (CV, measured in volts), the y-axis representing retention time (RT, measured in seconds), and the z-axis representing signal intensity (measured in volts). Raw data underwent standard chemometric preprocessing techniques, specifically baseline removal, as available in our previously reported AnalyzeIMS software [17-21], a custom software package to process and interpret differential mobility spectrometry data streams.

To quantify odorant concentration readings, the peak volume for each odorant compound (with a specific RT) was calculated by summing the signal corresponding to RT ± 10 s and CV values from −0.5 V to 0.5 V. The sensor was trained on n=3 samples of each mercaptan at five concentrations (0.1, 0.5, 1, 3, and 5 ppm). Linear regression was applied to the experimental data to obtain the calibration curve/model used to predict the compound concentration of natural gas samples. Once the required model parameters (slope and y-axis intercept) were obtained for each of the odorant compounds, the peak volumes of samples with unknown concentrations were fed into the model to predict the concentrations of individual odorant compounds.

3. Results and Discussion

3.1. Portable Analysis Platform Performance

3.1.1. Power Consumption—To gauge the power consumption of the device in practice, we attached a power meter (Kill A Watt® EZ, P3 International) to the device. Each run from sampling to completion averaged 30 Wh, this was limited by the resolution of the power meter. This is significantly lower than the power required to run a traditional GC analysis. With the low power requirements, it would be possible to run the device off a mobile generator or battery pack. For example, 500 Wh mobile battery packs are readily available for purchase and would be able to power the device to perform roughly 17 analysis runs.

3.1.2. Heat and Flow Control—Each of the heated devices followed a proportional control scheme for the pulse width modulated (PWM) control of the heater current but are capable of PID control with adjustments to the embedded code. The proportional gain results in supplying the full supply voltage to the heaters when temperature is below 4.1 °C of the target value and decreases PWM duty cycle linearly when temperature error smaller, which allowed the heated devices to heat up quickly and maintain stable temperature control at the target value. This is especially important for the trap which ideally would heat up as a step function to release the odorant compounds rapidly from the sorbent. Our implementation resulted in the trap reaching 90% of the target 150 °C within a mean time of 14 s (standard deviation, or SD=0.69). The heated devices also had very consistent temperature profiles throughout 25 runs during calibration curve data was obtained. Supplement plots of the 25 temperature profiles superimposed on a single set of axes visually confirms the repeatability of the temperature controls (S 8-1).

The control of flow rate proved to more of a challenge. PID closed-loop control was implemented for the proportional valves to augment the flow to track commanded flow

rates for the desorption flow and the carrier make up flow. There were several factors that contributed to the challenge of flow control for this system. The proportional valves used as the main actuator for the flow system had a non-linear response in a great portion of the minimum and maximum controllable range, as well as significant hysteresis during control direction changes. The needle valve was manually tuned to ensure the flow rates were achievable within the controllable operating range of the proportional valve. The resolution accuracy of the flow sensors was also an issue as we found there were inconsistencies with the readout of the flow sensors. Supplemental plots (S 8-2) of the device flow and pressure data show that the make-up flow was well controlled. There is significant high frequency variation seen in the plots of the desorption flow due to the combined factors of the flow sensor resolution at low flows and the limited control capabilities of the proportional valves. However, the average desorption flow over the course of an individual analysis followed the commanded values of 5 mL/min for desorption and 1 mL/min for GC column elution acceptably. The mean flow values for n=25: desorption 4.95 mL/min SD=0.48 and elution 1.01 mL/min SD=0.05.

For future work to improve the platform, there are several avenues to explore. One would be to decouple the desorption flow from the make-up flow. In this work, both controlled flows are derived from a single source flow. The source flow could be split but carries a tradeoff of requiring more components to isolate the two flows.

Despite the challenges, the flow system did perform consistently run to run with average flow values that matched the commanded values. More importantly, the application performance discussed in the following section shows the potential for this platform.

3.2. Application to Natural Gas Odorant Compounds

Prior to development of the sensor, a study was conducted to determine the appropriate sorbent material for the extraction and preconcentration of odorant compounds from natural gas. It was found that usage of the trap greatly increased detection sensitivity of the sulfur odorant compounds used in natural gas production and silica gel was the most sensitive as measured by signal per milligram sorbent. Additional details of this study are included as supplemental material (S5).

The detection and quantification capabilities of the platform were examined for a mixture of 6 mercaptan compounds found in three odorant blends commonly used in the natural gas industry (Spotleak 1009, 1039 and 1420). The six mercaptans included ethyl mercaptan (ETM), dimethyl sulfide (DMS), n-propyl mercaptan (NPM), iso-propyl mercaptan (IPM), tert-butyl mercaptan (TBM) and tetrahydrothiophene (THT). Figure 4 shows the detection signal from a synthetic sample containing all six mercaptans.

An example chromatograph is provided in Figure 4. Mercaptans were separated by the GC column, affording individual measurements and quantification of each compound. Peaks exhibited a symmetrical shape, with widths at half prominence ranging from 12.97 seconds (THT) to 36.25 seconds (TBM).

The first five eluting compounds (ETM, DMS, NPM, IPM and TBM) have very similar chemical structures and molecular weights; they elute at t=351, 386, 468, 581 and 653 s, respectively. This is highly conducive for in-field operations as analysis takes less than 11 minutes for these compounds, from sampling initiation to detection. Due to the high volatility of these mercaptans, a GC column with a strong sorbent coating was required to ensure separation, and ultimately the DB-624 coating used in this device GC column was appropriate. ETM and DMS, the first two eluting compounds, have slight peak overlap. At 3 ppm, the resolution (R) as calculated by **Equation 2** was 2.4, above the commonly accepted 1.2 value to ensure adequate peak separation for quantification (t_2 and t_1 are retention times of DMS and ETM, respectively; w is peak width at half height).

Because THT has a heavier molecular weight and different structure than the other mercaptans, it elutes later at t=1317 s. Heating the GC column from 40 °C to 160 °C, as incorporated in the device method, reduces the THT retention time than if the GC column were not heated, decreasing the total analysis time. For natural gas lines odorized with THT, the total analysis time is just under 22 minutes. There is work in the literature describing fast GC methods [22] that could be adapted to reduce the analysis time. The hardware development required to implement such methods could be explored in future works.

Calibration curve data for each mercaptan are presented in supplemental material (S9), which was trained on a randomized 60% of calibration samples. Specifically, three samples have been used to fit the calibration model and two samples have been used for the prediction purposes. The details of the obtained model are summarized in Table 1.

A linear response was observed for mercaptans as concentrations increased. Five compounds had high R^2 values, which ranged from 0.94 to 0.97. Dimethyl sulfide had an R^2 value of 0.79, and future work will aim to improve the linear response of DMS. The device reproducibility measured mercaptans (n=3): the average relative standard deviation to measure a given mercaptan at a given concentration was 4.9%, with a median of 5.1% and a range of 0.8% - 10.0%.

After calibration of the instrument, the remaining randomized 40% of the data was used to validate its performance. Samples were generated by spiking Tedlar bags with known concentrations of mercaptans with nitrogen balance gas. Figure 5 shows results for mercaptan concentration predictions against the actual mercaptan concentration of the sample. Higher error was observed for the lowest concentration, 0.1 ppm. This is likely due to the small signal generated by mercaptans at this concentration. Other factors could enhance detection of lower concentrations, such as increasing the sampling time; however, a target of 1 ppm was used herein. Excluding 0.1 ppm, the error observed ranged from 4.7 – 14.8% to accurately predict mercaptan concentrations. The intent of this device is to monitor mercaptan levels to ensure their presence is above a certain concentration in distribution lines. Overall, the system adequately predicted mercaptan concentrations in this proof-of-concept work. Future improvements to the system will be considered to further decrease measurement variability, however the device as is can be deployed to monitor mercaptan levels in the concentrations typically used in the industry.

We will further validate the platform under real world conditions, sampling natural gas from distribution lines and comparing our sensor readings against gold standard analytical measurements. While this was not within the scope of resources available work as presented, this follow up work is ongoing, and we anticipate a subsequent publication forthcoming.

4. Conclusions

A portable chemical detection platform was developed and demonstrated for monitoring odorant compounds in natural gas. This platform provides the means to perform on-site odorant concentration monitoring from sample-to-analysis and is the first of its kind to our knowledge. Several odorant compounds were successfully separated and detected at concentrations commonly encountered in the field. This success of this work shows great promise in advancing gas phase chemical separation and sensing beyond the confines of the laboratory environment. Future work will explore opportunities to adapt this platform to perform on-site analysis of volatiles in other fields.

Supplementary Material

Refer to Web version on PubMed Central for supplementary material.

Acknowledgements

The authors would like to thank Ahra Kwon for helpful discussions and natural gas industry insights. Zachary Carling, and Christina Zumout are thanked for their support of sample collection.

This work was primarily funded by the Northeast Gas Association (NGA). Periodically Northeast Gas Association sponsors product development and field-testing efforts providing funds or input for projects involving product specifications, design, prototype development, and laboratory or field testing. This activity is designed to assist the gas industry by providing new information to all interested parties. None of these entities participated in the planning, evaluation and analysis of the experimental data presented in this paper. Neither NGA, nor any of its members, warrant directly or indirectly, in any way or in any manner, that the reports, products, test results or information from these activities are accurate, effective or have application to the gas industry in any particular field setting, if at all. NGA, its members, and those acting on behalf of NGA, hereby expressly disclaim any and all liability, responsibility, damages or claims, of any kind or of any nature, that may result from use of these reports, products, test results, or information related thereto, does so at its own risk, without reliance on the fact that NGA and/or its members sponsored these activities. Such individual, corporation or other entity assumes any and all liability that may result from such use.

This research was funded in part under the Department of Transportation, Pipeline and Hazardous Materials Safety Administration's Pipeline Safety Research and Development Program, award 693JK32010008POTA [CED]. The views and conclusions contained in this document are those of the authors and should not be interpreted as representing the official policies, either expressed or implied, of the Pipeline and Hazardous Materials Safety Administration, or the U.S. Government.

This work was partially supported by: NIH awards 1U18TR003795, 4U18TR003795, 1U01TR004083; UL1 TR001860; UG3-OD023365; 1P30ES023513-01A1 [CED]; the Department of Veterans Affairs award I01 BX004965-01A1 [CED]; the University of California Tobacco-Related Disease Research Program award T31IR1614 [CED]; the National Science Foundation award 2200221 [CED]; student fellowship support from US Department of Education Award P200A180054 [DTK]; student fellowship support from NIH NHLBI award T32 HL07013 [BSC]; and Office of the Secretary of Defense and was accomplished under Agreement Number W911NF-17-3-0003 [CED]. This work was supported in part by the Laboratory Directed Research and Development program at Sandia National Laboratories, a multimission laboratory managed and operated by National Technology and Engineering Solutions of Sandia LLC, a wholly owned subsidiary of Honeywell International Inc. for the U.S. Department of Energy's National Nuclear Security Administration under contract DE-NA0003525 [CED].The contents of this manuscript are solely the responsibility of the authors and do not necessarily represent the official views of the funding agencies. The U.S. Government is authorized to reproduce and distribute reprints for Government purposes notwithstanding any copyright notation herein.

Part of this study was carried out at the UC Davis Center for Nano and Micro Manufacturing (CNM2).

7. References

[1]. U. Energy Information Administration, U.S. energy consumption by source and sector, 2021, 2022. https://www.eia.gov/totalenergy/data/monthly/pdf/flow/total-energy-spaghettichart-2021.pdf (accessed October 13, 2022).

[2]. Michanowicz DR, Dayalu A, Nordgaard CL, Buonocore JJ, Fairchild MW, Ackley R, Schiff JE, Liu A, Phillips NG, Schulman A, Magavi Z, Spengler JD, Home is Where the Pipeline Ends: Characterization of Volatile Organic Compounds Present in Natural Gas at the Point of the Residential End User, Environ Sci Technol. 56 (2022) 10258–10268. 10.1021/acs.est.1c08298. [PubMed: 35762409]

[3]. Solomon S, Qin D, Manning M, Chen Z, Marquis M, Averyt KB, Tignor M, Miller HL (eds.), IPCC (2007). Climate Change 2007: The Physical Science Basis, Cambridge, 2007. http://www.ipcc.ch/report/ar4/.

[4]. Kidnay AJ, Parrish WR, McCartney DG, Fundamentals of Natural Gas Processing: Second Edition, Fundamentals of Natural Gas Processing: Second Edition. (2011) 1–535. 10.1201/B14397/FUNDAMENTALS-NATURAL-GAS-PROCESSING-ARTHUR-KIDNAY-ARTHUR-KIDNAY-WILLIAM-PARRISH-DANIEL-MCCARTNEY.

[5]. Chevron Phillips Chemical, Odor-Fade Warning, (n.d.). https://web.archive.org/web/20230226205455/https://www.cpchem.com/odor-fade-warning (accessed February 25, 2023).

[6]. Sironi S, Capelli L, Haerens K, Segers P, Van Elst T, Sampling And Stability of Mercaptans: Comparison Between Bags, Canisters and Sorbent Tubes, Chem Eng Trans. 54 (2016). www.aidic.it/cet (accessed October 9, 2022).

[7]. de Angelis A, Natural gas removal of hydrogen sulphide and mercaptans, Appl Catal B. 113–114 (2012) 37–42. 10.1016/j.apcatb.2011.11.026.

[8]. Wilby FV, Variation in Recognition Odor Threshold of a Panel, J Air Pollut Control Assoc. 19 (1969) 96–100. 10.1080/00022470.1969.10466466.

[9]. Khan AM, Kallogjeri D, Piccirillo JF, Growing Public Health Concern of COVID-19 Chronic Olfactory Dysfunction, JAMA Otolaryngology–Head & Neck Surgery. 148 (2022) 81–82. 10.1001/JAMAOTO.2021.3379. [PubMed: 34792577]

[10]. Anishchenko IM, McCartney MM, Fung AG, Peirano DJ, Schirle MJ, Kenyon NJ, Davis CE, Modular and reconfigurable gas chromatography/differential mobility spectrometry (GC/DMS) package for detection of volatile organic compounds (VOCs), International Journal for Ion Mobility Spectrometry. 21 (2018) 125–136. 10.1007/s12127-018-0240-4. [PubMed: 31086501]

[11]. Hagemann LT, McCartney MM, Fung AG, Peirano DJ, Davis CE, Mizaikoff B, Portable combination of Fourier transform infrared spectroscopy and differential mobility spectrometry for advanced vapor phase analysis, Analyst. 143 (2018) 5683–5691. 10.1039/C8AN01192C. [PubMed: 30232480]

[12]. Luong J, Gras R, Mustacich R, Cortes H, Low Thermal Mass Gas Chromatography: Principles and Applications, J Chromatogr Sci. 44 (2006) 253–261. 10.1093/CHROMSCI/44.5.253. [PubMed: 16774710]

[13]. Miller RA, Eiceman GA, Nazarov EG, King AT, A novel micromachined high-field asymmetric waveform-ion mobility spectrometer, Sens Actuators B Chem. 67 (2000) 300–306. 10.1016/S0925-4005(00)00535-9.

[14]. Buryakov IA, Krylov EV, Nazarov EG, Rasulev U.Kh., A new method of separation of multi-atomic ions by mobility at atmospheric pressure using a high-frequency amplitude-asymmetric strong electric field, Int J Mass Spectrom Ion Process. 128 (1993) 143–148. 10.1016/0168-1176(93)87062-W.

[15]. Fung S, LeVasseur MK, Rajapakse MY, Chew BS, Fung AG, McCartney MM, Kenyon NJ, Davis CE, Battery powered dual-polarity ion detector for trace chemical sensing, Sens Actuators A Phys. 338 (2022) 113442. 10.1016/j.sna.2022.113442.

[16]. Pacific Gas and Electric Company, Sulfur Information, (n.d.). https://web.archive.org/web/20221006061407/https://www.pge.com/pipeline/operations/sulfur/sulfur_info/index.page (accessed February 16, 2023).

[17]. Peirano DJ, Pasamontes A, Davis CE, Supervised semi-automated data analysis software for gas chromatography / differential mobility spectrometry (GC/DMS) metabolomics applications, International Journal for Ion Mobility Spectrometry. 19 (2016) 155–166. 10.1007/S12127-016-0200-9/TABLES/1. [PubMed: 27799845]

[18]. Yeap D, McCartney MM, Rajapakse MY, Fung AG, Kenyon NJ, Davis CE, Peak detection and random forests classification software for gas chromatography/differential mobility spectrometry (GC/DMS) data, Chemometrics and Intelligent Laboratory Systems. 203 (2020) 104085. 10.1016/j.chemolab.2020.104085. [PubMed: 32801407]

[19]. Chakraborty P, Rajapakse MY, McCartney MM, Kenyon NJ, Davis CE, Machine learning and signal processing assisted differential mobility spectrometry (DMS) data analysis for chemical identification, Analytical Methods. 14 (2022) 3315–3322. 10.1039/D2AY00723A. [PubMed: 35968834]

[20]. Rajapakse MY, Borras E, Yeap D, Peirano DJ, Kenyon NJ, Davis CE, Automated chemical identification and library building using dispersion plots for differential mobility spectrometry, Analytical Methods. 10 (2018) 4339–4349. 10.1039/C8AY00846A. [PubMed: 30984293]

[21]. Yeap D, Hichwa PT, Rajapakse MY, Peirano DJ, McCartney MM, Kenyon NJ, Davis CE, Machine Vision Methods, Natural Language Processing, and Machine Learning Algorithms for Automated Dispersion Plot Analysis and Chemical Identification from Complex Mixtures, Anal Chem. 91 (2019) 10509–10517. 10.1021/acs.analchem.9b01428. [PubMed: 31310101]

[22]. Zoccali M, Tranchida PQ, Mondello L, Fast gas chromatography-mass spectrometry: A review of the last decade, TrAC Trends in Analytical Chemistry. 118 (2019) 444–452. 10.1016/j.trac.2019.06.006.

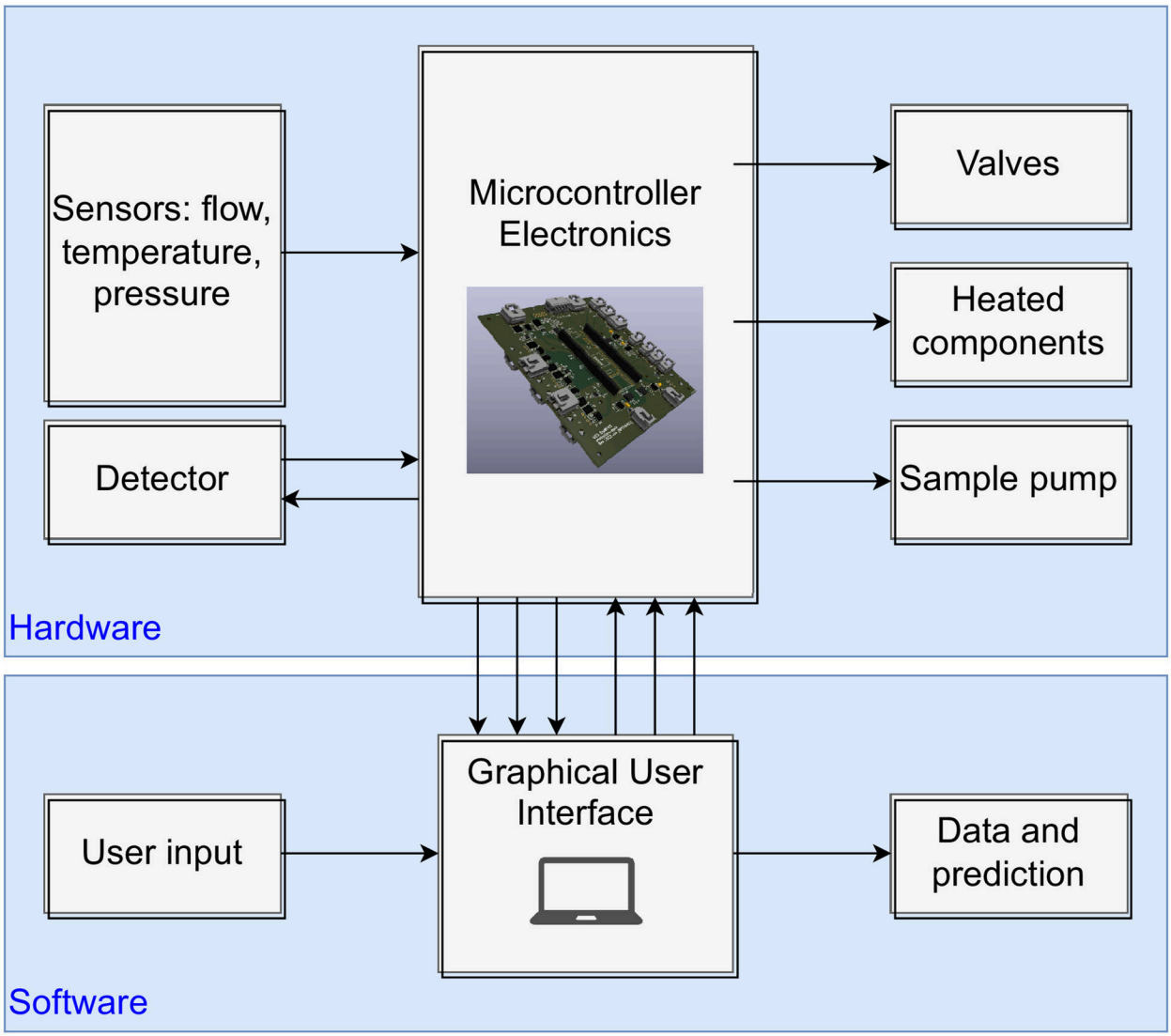

Figure 1.
Overall platform architecture. The arrows show the general flow of data and control. As inputs, the microcontroller takes sensor and detector data. As outputs, the microcontroller communicates with the detector and controls system hardware including valves, heated components, and the sample pump. The Graphical User Interface program takes user input for method parameters while saving data and providing compound prediction capabilities.

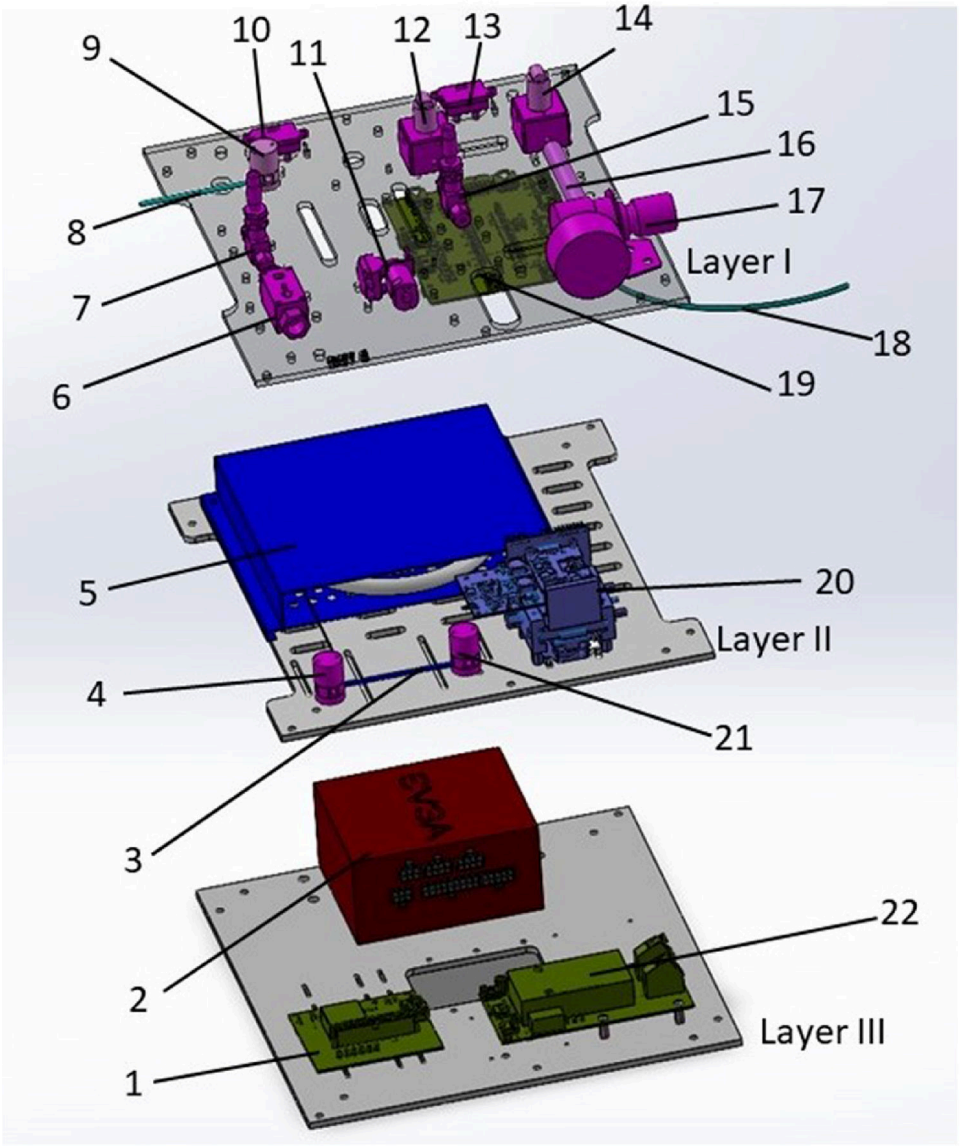

Figure 2.

The device is divided into 3 stacked layers in a custom acrylic housing – **Layer I**: flow control, **Layer II**: analysis, **Layer III**: power. The parts are numbered as follows: **1** main power electronics; **2** device power supply; **3** silica gel trap; **4, 9, 21** 2-way valves; **5** GC; **6** natural gas sample flow sensor; **7, 15** needle valve; **8** sample inlet; **10, 13** flow sensors; **11** sample pump; **12, 14** proportional valve; **16** filter; **17** nitrogen pressure regulator; **18** nitrogen inlet; **19** device control electronics; **20** differential mobility spectrometer detector; **22** ionization power electronics. Components are color coded – purple: flow, green: electronics, blue: analysis.

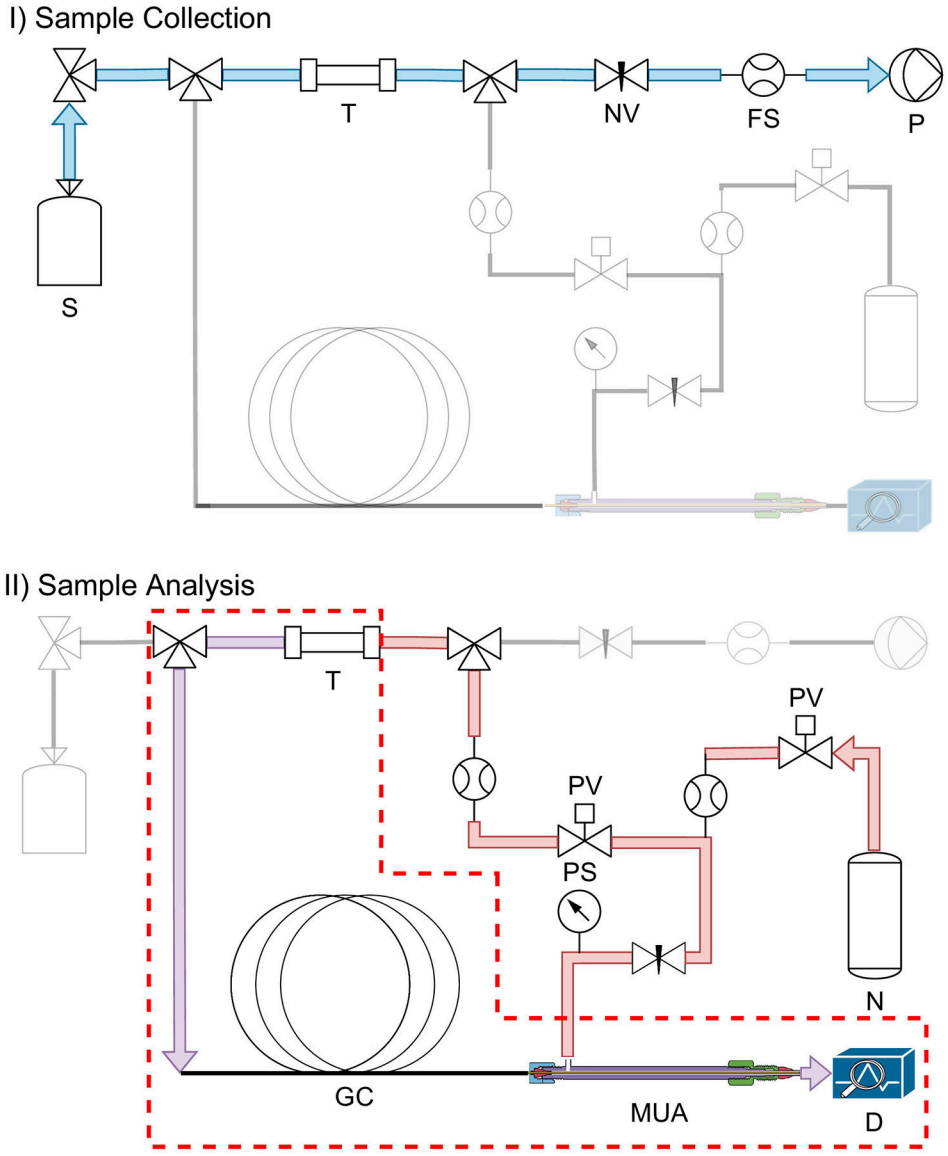

Figure 3.

Hardware schematic. I) Sample flow path is light blue. II) Nitrogen flow is light red. Sample flow carried by nitrogen is violet. Active heating is indicated by the dashed line. Legend: **S** sample inlet; **T** silica gel trap; **NV** needle valve; **FS** flow sensor; **P** sample pump; **PV** proportional valve; **PS** pressure sensor; **N** nitrogen; **GC** gas chromatography column; **MUA** make-up adapter; **D** detector.

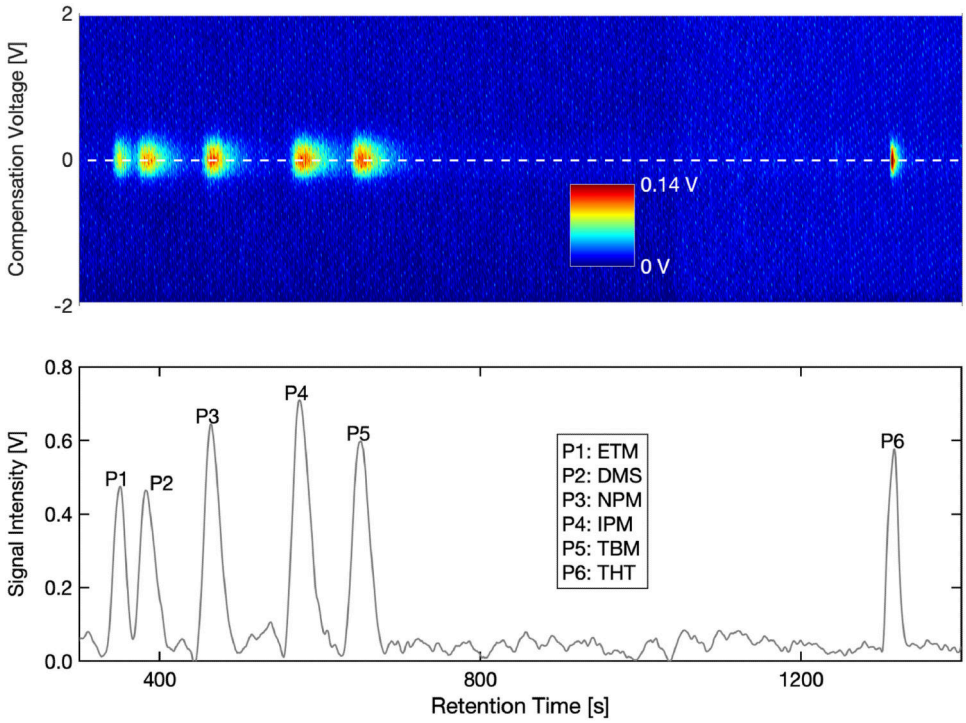

Figure 4.

Detection signal from a sample containing the six mercaptan analytes. (top) Raw signal, showing the three dimensionality of the detector data (bottom) Side view of the detector data.

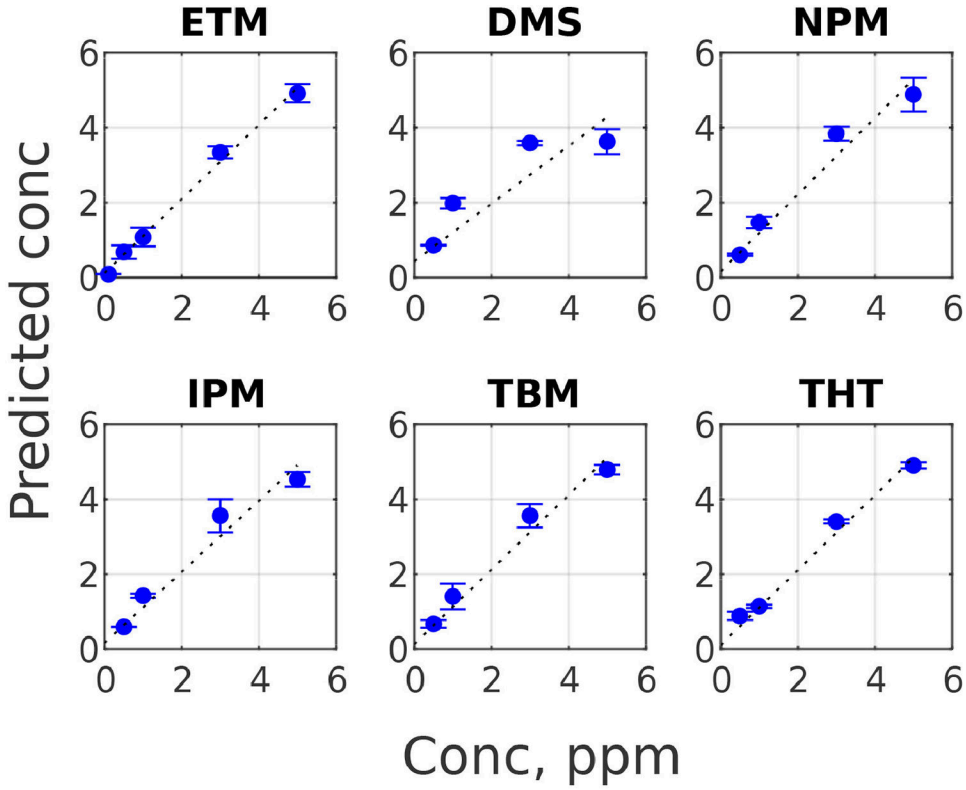

Figure 5.
Predictions of mercaptan concentrations (conc) from a sample (y-axis) against the actual mercaptan concentration (x-axis).

Table 1:

Linear calibration model parameters for predicting the mercaptan concentration in the samples

	Slope of the linear model (m)	Y-axis intercept of the linear model (c)	R-squared value
ETM	1.03	−1.65	0.99
DMS	1.42	−2.9	0.81
NPM	0.92	−1.77	0.96
IPM	0.91	−1.83	0.94
TBM	0.96	−1.86	0.96
THT	0.98	−1.99	0.97